Magnetic Dipolar Interaction between Hyperfine Clock States in a Planar Alkali Bose Gas

Y.-Q. Zou, B. Bakkali-Hassani, C. Maury, É. Le Cerf, S. Nascimbene, J. Dalibard, and J. Beugnon*
Laboratoire Kastler Brossel, Collège de France, CNRS, ENS-PSL University, Sorbonne Université, 11 Place Marcelin Berthelot, 75005 Paris, France

(Received 28 July 2020; accepted 4 November 2020; published 2 December 2020)

In atomic systems, clock states feature a zero projection of the total angular momentum and thus a low sensitivity to magnetic fields. This makes them widely used for metrological applications like atomic fountains or gravimeters. Here, we show that a mixture of two such nonmagnetic states still displays magnetic dipole-dipole interactions comparable to the one expected for the other Zeeman states of the same atomic species. Using high-resolution spectroscopy of a planar gas of ^{87}Rb atoms with a controlled in plane shape, we explore the effective isotropic and extensive character of these interactions and demonstrate their tunability. Our measurements set strong constraints on the relative values of the s-wave scattering lengths a_{ij} involving the two clock states.

DOI: 10.1103/PhysRevLett.125.233604

Quantum atomic gases constitute unique systems to investigate many-body physics thanks to the precision with which one can control their interactions [1,2]. Usually, in the ultralow temperature regime achieved with these gases, contact interactions described by the s-wave scattering length dominate. In recent years, nonlocal interaction potentials have been added to the quantum gas toolbox. Long-range interactions can be mediated thanks to optical cavities inside which atoms are trapped [3]. Electric dipole-dipole interactions are routinely achieved via excitation of atoms in Rydberg electronic states [4]. Atomic species with large magnetic moments in the ground state, like Cr, Er, or Dy, offer the possibility to explore the role of magnetic dipole-dipole interactions (MDDIs) [5]. The latter case has led, for instance, to the observation of quantum droplets [6], roton modes [7], or spin dynamics in lattices with off site interactions [8–10].

For alkali-metal atoms, which are the workhorse of many cold-atom experiments, the magnetic moment is limited to $\lesssim 1$ Bohr magneton (μ_B) and in most cases, MDDIs have no sizeable effect on the gas properties [11]. However, some paths have been investigated to evidence their role also for these atomic species. A first route consists of specifically nulling the s-wave scattering length using a Feshbach resonance [12,13], so that MDDIs become dominant. A second possibility is to operate with a multicomponent (or spinor) gas [14], using several states from the ground-level manifold of the atoms. One can then take advantage of a possible coincidence of the various scattering lengths in play. When it occurs, the spin-dependent contact interaction is much weaker than the spin-independent one, and MDDIs can have a significant effect [15], e.g., on the generation of spin textures [16,17] and on magnon spectra [18]. In all instances studied so far with these multicomponent gases, each component possesses a nonzero magnetic moment and creates a magnetic field that influences its own dynamics, as well as the dynamics of the other component(s).

In this Letter, we present another, yet unexplored, context in which MDDIs can influence significantly the physics of a two-component gas of alkali-metal atoms. We operate with a superposition of the two hyperfine states of ^{87}Rb involved in the so-called hyperfine clock transition, $|1\rangle \equiv |F = 1, m_Z = 0\rangle$ and $|2\rangle \equiv |F = 2, m_Z = 0\rangle$, where the quantization axis Z is aligned with the uniform external magnetic field [Fig. 1(a)]. For a single-component gas prepared in one of these two states, the average magnetization is zero by symmetry and MDDIs have no effect. However, when atoms are simultaneously present in these two states, we show that magnetic interactions between them are nonzero, and that the corresponding MDDIs can modify significantly the position of the clock transition frequency.

Our Letter constitutes a magnetic analog of the observation of electric dipole-dipole interactions (EDDIs) between molecules in a Ramsey interferometric scheme [19]. There, in spite of the null value of the electric dipole moment of a molecule prepared in an energy eigenstate, it was shown that EDDIs can be induced in a molecular gas by preparing a coherent superposition of two rotational states. Both in our Letter and in [19], the coupling between two partners results in a pure exchange interaction, with one partner switching from $|1\rangle$ to $|2\rangle$ and the other one from $|2\rangle$ to $|1\rangle$. This exchange Hamiltonian also appears for resonant EDDIs between atoms prepared in different Rydberg states [20].

In spite of their different origin, the physical manifestations of MDDIs in our setup are similar to the standard ones. Here, we study it for a 2D gas using high-resolution Ramsey spectroscopy [Fig. 1(b)] and we explicitly test two important features of dipole-dipole interactions in this

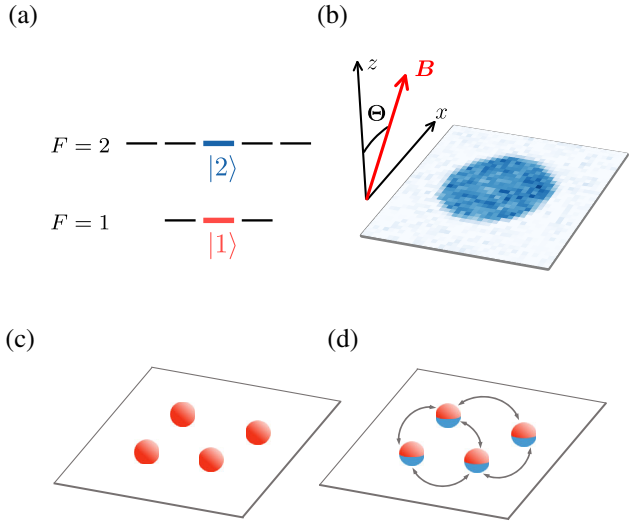

FIG. 1. (a) Level diagram of the hyperfine ground-level manifold showing the two states relevant to this Letter: $|1\rangle \equiv |F = 1, m_Z = 0\rangle$ and $|2\rangle \equiv |F = 2, m_Z = 0\rangle$. (b) Image of the atomic cloud obtained through absorption imaging along the direction perpendicular to the atomic plane. Atoms are confined in the xy plane in a disk of radius 12 μm. The orientation of the magnetic field $\boldsymbol{B}$ is tuned in the xz plane. (c) Schematics of atoms prepared in the state $|1\rangle$, with no MDDIs in this case. MDDIs are also absent when all atoms are in $|2\rangle$. (d) Significant MDDIs occur for atoms in a linear superposition of $|1\rangle$ and $|2\rangle$.

planar geometry: their effect does not depend on the in plane shape of the cloud (isotropy), nor on its size (extensivity). More precisely, we recast the role of MDDIs as a modification of the s-wave interspecies scattering length a_{12} and show the continuous tuning of a_{12} by changing the orientation of the external magnetic field with respect to the atom plane. We obtain in this way accurate information on the relative values of intra- and interspecies bare scattering lengths of the studied states.

We start with the restriction of the MDDIs Hamiltonian to the clock state manifold [21], using the magnetic interaction between two electronic spins $\hat{\boldsymbol{s}}_A$ and $\hat{\boldsymbol{s}}_B$ with magnetic moments $\boldsymbol{m}_{A,B} = 2\mu_B \boldsymbol{s}_{A,B}$,

$$\hat{V}_{dd}(r, \boldsymbol{u}) = \frac{\mu_0 \mu_B^2}{\pi r^3}[\hat{\boldsymbol{s}}_A \cdot \hat{\boldsymbol{s}}_B - 3(\hat{\boldsymbol{s}}_A \cdot \boldsymbol{u})(\hat{\boldsymbol{s}}_B \cdot \boldsymbol{u})], \quad (1)$$

where r is the distance between the two dipoles and $\boldsymbol{u}$ is the unit vector connecting them. The calculation detailed in the Supplemental Material [22] shows that MDDIs do not modify the interactions between atoms in the same state $|1\rangle$ or $|2\rangle$, but induce a nonlocal, angle-dependent exchange interaction [Figs. 1(c) and 1(d)]. The second-quantized Hamiltonian of the MDDIs for the clock states is thus

$$\hat{H}_{dd}^{(1,2)} = \frac{\mu_0 \mu_B^2}{4\pi} \iint d^3 r_A d^3 r_B \frac{1 - 3\cos^2\theta}{r^3} \times \hat{\Psi}_2^\dagger(\boldsymbol{r}_A)\hat{\Psi}_1^\dagger(\boldsymbol{r}_B)\hat{\Psi}_2(\boldsymbol{r}_B)\hat{\Psi}_1(\boldsymbol{r}_A), \quad (2)$$

where the $\hat{\Psi}_i(\boldsymbol{r}_\alpha)$ are the field operators annihilating a particle in state $|i\rangle$ at position $\boldsymbol{r}_\alpha$, $r = |\boldsymbol{r}_A - \boldsymbol{r}_B|$, and θ is the angle between $\boldsymbol{r}_A - \boldsymbol{r}_B$ and the quantization axis.

We now investigate the spatial average value of $\hat{H}_{dd}^{(1,2)}$. We note first that, for a 3D isotropic gas, the angular integration gives $\langle \hat{H}_{dd}^{(1,2)} \rangle_{3D} = 0$, as usual for MDDIs [5]. We then consider a homogeneous quasi-2D Bose gas confined isotropically in the xy plane with area L^2. We assume that the gas has a Gaussian density profile along the third direction z, $n_{1,2}(z) = N_{1,2} e^{-z^2/\ell_z^2}/\sqrt{\pi}\ell_z L^2$, where $\ell_z = \sqrt{\hbar/m\omega_z}$ is the extension of the ground state of the harmonic confinement of frequency ω_z for particles of mass m, and $N_{1,2}$ is the atom number in states $|1\rangle$, $|2\rangle$. One then finds [23–25]

$$\langle \hat{H}_{dd}^{(1,2)} \rangle_{2D} = \frac{\mu_0 \mu_B^2 N_1 N_2}{3\sqrt{2\pi}\ell_z L^2}(3\cos^2\Theta - 1), \quad (3)$$

where Θ is the angle between the external magnetic field $\boldsymbol{B}$ and the direction perpendicular to the atomic plane. This energy is maximal and positive for $\boldsymbol{B}$ perpendicular to the atomic plane ($\Theta = 0$) and minimal and negative for $\boldsymbol{B}$ in the atomic plane ($\Theta = \pi/2$). Equation (3) shows that the energy per atom in state $|1\rangle$ depends only on the spatial density N_2/L^2 of atoms in state $|2\rangle$, which proves the extensivity.

In 2D, the Fourier transform of the dipole-dipole Hamiltonian possesses a well-defined value at the origin $\boldsymbol{k} = 0$ [23]. Consequently, for a large enough sample (typically, $L \gg \ell_z$), the average energy $\langle \hat{H}_{dd}^{(1,2)} \rangle_{2D}$, evaluated by switching the integral (2) to Fourier space, is independent of the system shape. This contrasts with the 3D case, for which the MDDIs energy changes sign when switching from an oblate to a prolate cloud [5,26]. Considering the effective isotropy of the MDDIs in this 2D configuration, it is convenient to describe their role as a change δa_{12} of the interspecies scattering length with respect to its bare value defined as $a_{12}^{(0)}$. In 2D, interspecies contact interactions lead to $\langle \hat{H}_{\text{contact}}^{(1,2)} \rangle_{2D} = \sqrt{8\pi} a_{12} \hbar^2 N_1 N_2/(m\ell_z L^2)$ and we deduce

$$\delta a_{12}(\Theta) = a_{dd}(3\cos^2\Theta - 1), \quad (4)$$

where $a_{dd} = \mu_0 \mu_B^2 m/(12\pi\hbar^2)$ is the so-called dipole length that quantifies the strength of MDDIs [27].

We now tackle the experimental observation of this modification of the interspecies scattering length in a quasi-2D Bose gas. The experimental setup was described in [30,31]. Basically, a cloud of ^{87}Rb atoms in state $|1\rangle$ is confined in a 2D box potential: A "hard-wall" potential provides a uniform in plane confinement inside a 12 μm radius disk, unless otherwise stated. The vertical confinement can be approximated by a harmonic potential

with frequency $\omega_z/2\pi = 4.4(1)$ kHz, corresponding to $\ell_z = 160$ nm. We operate in the weakly interacting regime characterized by the dimensionless coupling constant $\tilde{g} = \sqrt{8\pi}a_{11}/\ell_z = 0.16(1)$, where a_{11} is the s-wave scattering length for atoms in $|1\rangle$. The in plane density of the cloud is $\bar{n} \approx 95/\mu\text{m}^2$ and we operate at the lowest achievable temperature in our setup $T < 30$ nK. A ≈ 0.7 G bias magnetic field $\boldsymbol{B}$ with tunable orientation is fixed during the experiment.

Spectroscopy is performed thanks to a Ramsey sequence similar to [32]. Atoms initially in $|1\rangle$ are coupled to state $|2\rangle$ with a microwave field tuned around the hyperfine splitting of 6.8 GHz. A first Ramsey pulse with a typical duration of a few tens of microseconds, creates a superposition of the two clock states with a tunable weight. After an "interrogation time" $T_R = 10$ ms, a second identical Ramsey pulse is applied [33]. After this second pulse, we perform absorption imaging to determine the population in $|2\rangle$. We measure the variation of this population as a function of the frequency of the microwave field, see Figs. 2(a) and 2(b). We fit a sinusoidal function to the data, so as to determine the resonance frequency of the atomic cloud. All frequency measurements $\Delta\nu$ are reported with respect to reference measurements of the single-atom response that we perform on a dilute cloud. The typical dispersion of the measurement of this single-atom response is about 1 Hz and provides an estimate of our uncertainty on the frequency measurements. We checked that the measured resonance frequencies are independent of T_R in the range 5–20 ms. Shorter delays lead to a lower accuracy on the frequency measurement. For longer delays, we observe demixing dynamics [34] between the two components and a modification of the resonance frequency.

In the following, we restrict to the case of strongly degenerate clouds [35] described in the mean-field approximation. Consider first the case of a uniform 3D gas. The resonant frequency $\Delta\nu$ can be computed by evaluating the difference of mean-field shifts for the two components [32],

$$\Delta\nu = \frac{\hbar}{m} n[a_{22} - a_{11} + (2a_{12} - a_{11} - a_{22})f]. \qquad (5)$$

Here the a_{ij} are the inter- and intraspecies scattering lengths, $n = n_1 + n_2$ is the total 3D density of the cloud where each component i has a density n_i after the first Ramsey pulse and $f = (n_1 - n_2)/(n_1 + n_2)$ describes the population imbalance between the two states.

It is interesting to discuss briefly two limiting cases of Eq. (5). In the low transfer limit $f \approx 1$, the first Ramsey pulse produces only a few atoms in state $|2\rangle$, imbedded in a bath of state $|1\rangle$ atoms. Interactions within pairs of state $|2\rangle$ atoms then play a negligible role, so that the shift $\Delta\nu$ does not depend on a_{22}. It is proportional to $(a_{12} - a_{11})$, hence sensitive to MDDIs. In the balanced case $f = 0$, the Ramsey sequence transforms a gas initially composed only of atoms in state $|1\rangle$ into a gas composed only of atoms in state $|2\rangle$. The energy balance between initial and final states then gives a contribution $\Delta\nu \propto (a_{22} - a_{11})$, which is insensitive to MDDIs.

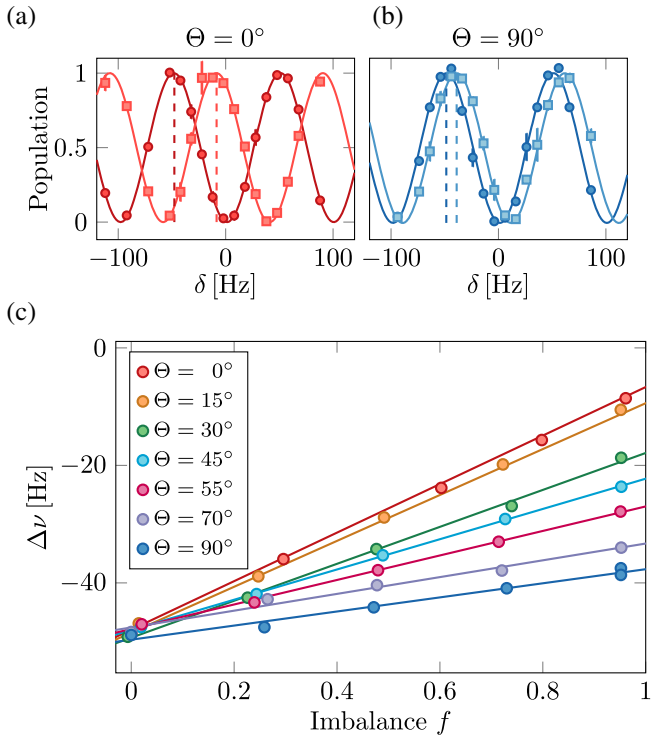

FIG. 2. (a),(b) Normalized Ramsey oscillations measured for $\boldsymbol{B}$ perpendicular ($\Theta = 0°$) or parallel ($\Theta = 90°$) to the atomic plane. For both cases, we show the transferred population as a function of detuning δ to the single-atom resonance. In each case the resonance is marked by a vertical dashed line. The circles (respectively, squares) correspond to a balanced (respectively, unbalanced) mixture $f = 0$ (respectively, $f \approx 0.95$). Vertical error bars represent the standard deviation from the two measurements realized for each points. (c) Variation of the frequency shift $\Delta\nu$ with the imbalance f. We restrict to positive imbalances, for which the population in $|2\rangle$ remains small enough to limit the role of two-body relaxation and spin-changing collisions. For each angle, the solid line is a linear fit to the data.

It is important to note that the validity of Eq. (5) for a many-body system is not straightforward and requires some care [36,37]. We discuss in Ref. [38] the applicability of this approach to our experimental system and show that it relies on the almost equality of the three relevant scattering lengths a_{ij} of the problem. Note also that in our geometry, even if the gas is uniform in plane, the density distribution along z is inhomogeneous and the spectroscopy measurement is thus sensitive to the integrated density $\bar{n}(x, y) = \int dz n(x, y, z)$.

We now discuss the measurement of the frequency shift $\Delta\nu$ as a function of the imbalance f for different orientations of the magnetic field with respect to the atomic plane, see Fig. 2(c). For each orientation, we confirm the linear behavior expected from Eq. (5). The variation of the slope

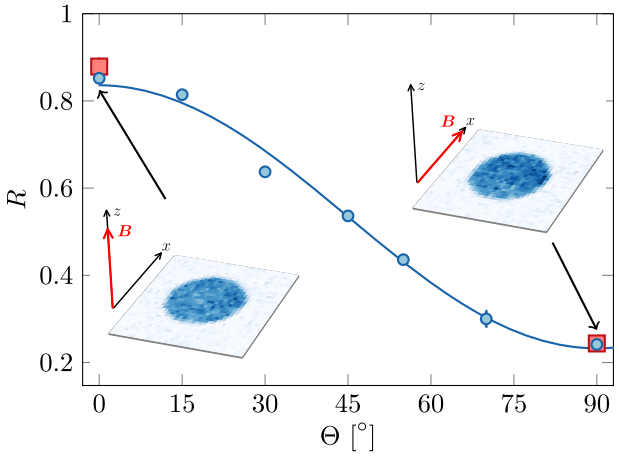

FIG. 3. Variation of the ratio $R(\Theta)$ determined from the data of Fig. 2(c) with the magnetic field orientation Θ. Blue circles (respectively, red squares) correspond to the measurement at maximum density (respectively, half density). The variation of this ratio is well fitted by a cosine variation compatible with the prediction for MDDIs. The amplitude and offset of this variation allow one to determine accurately relative values of the scattering lengths. Vertical error bars represent the uncertainty obtained from the fitting procedure of the data in Fig. 2. The uncertainty on the determination of the angles is limited by the geometrical arrangement of the coils generating the field $\boldsymbol{B}$, estimated here at the level of 1°.

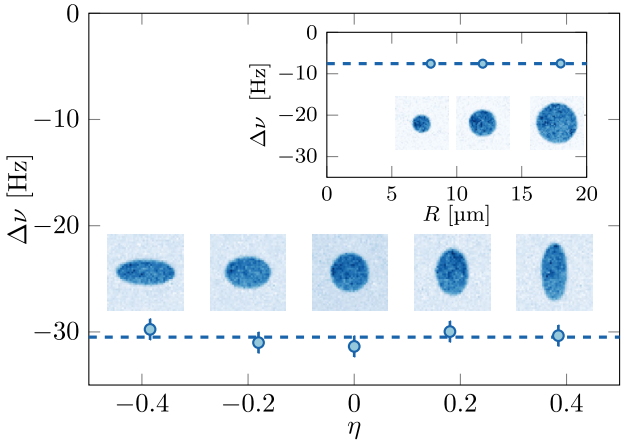

FIG. 4. Interaction shift $\Delta\nu$ as a function of the anisotropy parameter η. For a fixed density and an in plane magnetic field, we vary the anisotropy of the elliptically shaped 2D cloud. No dependence on the shape of the cloud is observed, in agreement with the expected isotropic character of MDDIs in 2D when $R_{x,y} \gg \ell_z$. Vertical error bars represent the estimated 1 Hz accuracy on the determination of the single-atom resonance frequency. Inset: interaction shift as a function of the size of the cloud, for $\boldsymbol{B}$ normal to the atom plane.

$d\Delta\nu/df$ for different orientations reflects the expected modification of a_{12} with Θ of Eq. (4). More quantitatively, we fit a linear function to the data for each Θ. The ratio of the slope to the intercept of this line is $R(\Theta) = [a_{22} + a_{11} - 2a_{12}(\Theta)]/(a_{22} - a_{11})$. Interestingly, this ratio is independent of the density calibration and is thus a robust observable.

The evolution of the measured ratio for different angles is shown in Fig. 3. For $\Theta = 0°$ and 90°, we also show the ratio measured for a density approximately twice as small as the one of Fig. 2. These two points overlap well with the main curve, which confirms the insensitivity of R with respect to $\bar{n}$. We fit a sinusoidal variation $\Theta \mapsto \alpha + \beta\cos(2\Theta)$ to $R(\Theta)$ from which we extract $\alpha = 0.53(1)$ and $\beta = 0.30(1)$. We then determine $a_{22} - a_{11} = -3a_{dd}/\beta$ and $a_{12}^{(0)} - a_{11} = a_{dd}(3\alpha - 3 - \beta)/(2\beta)$. Using $a_{dd} = 0.70a_0$, with a_0 the Bohr radius, we find $a_{22} - a_{11} = -7.0(2)a_0$ and $a_{12}^{(0)} - a_{11} = -2.0(1)a_0$. These results are in good agreement with the values predicted in [39], $a_{11} = 100.9a_0$, $a_{22} - a_{11} = -6.0a_0$, and $a_{12}^{(0)} - a_{11} = -2.0a_0$.

All experiments described so far have been realized with a fixed disk geometry. As stated above, the description of the contribution of MDDIs as a modification of the interspecies scattering length relies on the effective isotropy of the interaction in our 2D system. We investigate this issue by measuring the frequency shift of the clock transition for an in plane magnetic field orientation ($\Theta = 90°$), which breaks the rotational symmetry of the system. We operate with a fixed density ($\bar{n} \approx 80/\mu\text{m}^2$) and a varying elliptical shape. We choose a large imbalance $f \approx 0.95$ to have the highest sensitivity to possible modifications of a_{12}. We define an anisotropy parameter $\eta = (R_y - R_x)/(R_x + R_y)$ for the ratio of the lengths R_x and R_y of the two axes of the ellipse. We report in Fig. 4 the measured shifts as a function of η and confirm, within our experimental accuracy, the independence of the MDDIs energy with respect to the cloud shape. We have also investigated the influence of the size of the cloud on $\Delta\nu$ (inset of Fig. 4). Here we choose a disk-shaped cloud and a magnetic field perpendicular to the atomic plane. We observe no detectable change of $\Delta\nu$ when changing the disk radius from 8 to 18 μm, which confirms the absence of significant finite-size effects.

In conclusion, thanks to high-resolution spectroscopy we revealed the non-negligible role of magnetic dipolar interactions between states with a zero average magnetic moment. We observed and explained the modification of the interspecies scattering length in a two-component cloud. Because of the smallness of MDDIs for alkali-metal atoms, we did not observe any modification of the global shape of the cloud. This contrasts with the case of single-component highly magnetic dipolar gases where the shape of a trapped gas has been modified with a static [40–42] or time-averaged-field [11,43]. Nevertheless, the effect observed here provides a novel control on the dynamics of two-component gases. For example, the effective interaction parameter between two atoms in state $|2\rangle$ mediated by a bath of atoms in state $|1\rangle$ can be written as

$\tilde{g}_{22}^{\mathrm{eff}} = \tilde{g}_{22} - \tilde{g}_{12}^2/\tilde{g}_{11}$, where $\tilde{g}_{ij} = \sqrt{8\pi}a_{ij}/\ell_z$ [44]. With our parameters, we achieve a variation by a factor 7 of $\tilde{g}_{22}^{\mathrm{eff}}$, which will lead to important modifications of polaron dynamics. Similarly, it can be exploited to tune the miscibility of mixtures or the dynamics of spin textures. The distance to the critical point for miscibility, whose position is given by $\tilde{g}_{22}\tilde{g}_{11} = \tilde{g}_{12}^2$, is also strongly sensitive to a variation of $\tilde{g}_{12}$. For instance, the length scale of spin textures appearing in phase separation dynamics of a balanced mixture will be modified, for our parameters, by a factor of almost 3 when Θ is switched from 0° to 90° [34]. In addition, one can exploit the nonlocal character of MDDIs by confining the atoms in a deep lattice at unit filling, where the exchange coupling evidenced here will implement the so-called quantum XX model [45] without requiring any tunneling between lattice sites. The extreme sensitivity of the clock transition and its protection from magnetic perturbations will then provide a novel, precise tool to detect the various phases of matter predicted within this model.

This work is supported by ERC (Synergy UQUAM), European Union's Horizon 2020 Programme (QuantERA-NAQUAS project), and the ANR-18-CE30-0010 grant. We thank F. Pereira dos Santos, M. Zwierlein, and P. Julienne for stimulating discussions. We acknowledge the contribution of R. Saint-Jalm at the early stage of the project.

*beugnon@lkb.ens.fr

[1] C. Chin, R. Grimm, P. Julienne, and E. Tiesinga, Feshbach resonances in ultracold gases, Rev. Mod. Phys. **82**, 1225 (2010).
[2] I. Bloch, J. Dalibard, and W. Zwerger, Many-body physics with ultracold gases, Rev. Mod. Phys. **80**, 885 (2008).
[3] K. Baumann, C. Guerlin, F. Brennecke, and T. Esslinger, Dicke quantum phase transition with a superfluid gas in an optical cavity, Nature (London) **464**, 1301 (2010).
[4] R. Löw, H. Weimer, J. Nipper, J. B. Balewski, B. Butscher, H. P. Büchler, and T. Pfau, An experimental and theoretical guide to strongly interacting Rydberg gases, J. Phys. B **45**, 113001 (2012).
[5] T. Lahaye, C. Menotti, L. Santos, M. Lewenstein, and T. Pfau, The physics of dipolar bosonic quantum gases, Rep. Prog. Phys. **72**, 126401 (2009).
[6] I. Ferrier-Barbut, H. Kadau, M. Schmitt, M. Wenzel, and T. Pfau, Observation of Quantum Droplets in a Strongly Dipolar Bose Gas, Phys. Rev. Lett. **116**, 215301 (2016).
[7] L. Chomaz, R. M. W. van Bijnen, D. Petter, G. Faraoni, S. Baier, J. H. Becher, M. J. Mark, F. Waechtler, L. Santos, and F. Ferlaino, Observation of Roton mode population in a dipolar quantum gas, Nat. Phys. **14**, 442 (2018).
[8] A. de Paz, A. Sharma, A. Chotia, E. Maréchal, J. H. Huckans, P. Pedri, L. Santos, O. Gorceix, L. Vernac, and B. Laburthe-Tolra, Nonequilibrium Quantum Magnetism in a Dipolar Lattice Gas, Phys. Rev. Lett. **111**, 185305 (2013).
[9] S. Baier, M. J. Mark, D. Petter, K. Aikawa, L. Chomaz, Z. Cai, M. Baranov, P. Zoller, and F. Ferlaino, Extended Bose-Hubbard models with ultracold magnetic atoms, Science **352**, 201 (2016).
[10] S. Lepoutre, J. Schachenmayer, L. Gabardos, B. Zhu, B. Naylor, E. Maréchal, O. Gorceix, A. M. Rey, L. Vernac, and B. Laburthe-Tolra, Out-of-equilibrium quantum magnetism and thermalization in a spin-3 many-body dipolar lattice system, Nat. Commun. **10**, 1714 (2019).
[11] S. Giovanazzi, A. Görlitz, and T. Pfau, Tuning the Dipolar Interaction in Quantum Gases, Phys. Rev. Lett. **89**, 130401 (2002).
[12] M. Fattori, G. Roati, B. Deissler, C. D'Errico, M. Zaccanti, M. Jona-Lasinio, L. Santos, M. Inguscio, and G. Modugno, Magnetic Dipolar Interaction in a Bose-Einstein Condensate Atomic Interferometer, Phys. Rev. Lett. **101**, 190405 (2008).
[13] S. E. Pollack, D. Dries, M. Junker, Y. P. Chen, T. A. Corcovilos, and R. G. Hulet, Extreme Tunability of Interactions in a ^{7}Li Bose-Einstein Condensate, Phys. Rev. Lett. **102**, 090402 (2009).
[14] D. M. Stamper-Kurn and M. Ueda, Spinor Bose gases: Symmetries, magnetism, and quantum dynamics, Rev. Mod. Phys. **85**, 1191 (2013).
[15] S. Yi, L. You, and H. Pu, Quantum Phases of Dipolar Spinor Condensates, Phys. Rev. Lett. **93**, 040403 (2004).
[16] M. Vengalattore, S. R. Leslie, J. Guzman, and D. M. Stamper-Kurn, Spontaneously Modulated Spin Textures in a Dipolar Spinor Bose-Einstein Condensate, Phys. Rev. Lett. **100**, 170403 (2008).
[17] Y. Eto, H. Saito, and T. Hirano, Observation of Dipole-Induced Spin Texture in an ^{87}Rb Bose-Einstein Condensate, Phys. Rev. Lett. **112**, 185301 (2014).
[18] G. E. Marti, A. MacRae, R. Olf, S. Lourette, F. Fang, and D. M. Stamper-Kurn, Coherent Magnon Optics in a Ferromagnetic Spinor Bose-Einstein Condensate, Phys. Rev. Lett. **113**, 155302 (2014).
[19] B. Yan, S. A. Moses, B. Gadway, J. P. Covey, K. R. A. Hazzard, A. M. Rey, D. S. Jin, and J. Ye, Observation of dipolar spin-exchange interactions with lattice-confined polar molecules, Nature (London) **501**, 521 (2013).
[20] S. de Léséleuc, D. Barredo, V. Lienhard, A. Browaeys, and T. Lahaye, Optical Control of the Resonant Dipole-Dipole Interaction between Rydberg Atoms, Phys. Rev. Lett. **119**, 053202 (2017).
[21] For all experiments reported here, the fraction of atoms in any other spin state remains below our detection sensitivity of 1%.
[22] See Supplemental Material at http://link.aps.org/supplemental/10.1103/PhysRevLett.125.233604 for details on the calculation of the effective interspecies scattering length a_{12}.
[23] U. R. Fischer, Stability of quasi-two-dimensional Bose-Einstein condensates with dominant dipole-dipole interactions, Phys. Rev. A **73**, 031602(R) (2006).
[24] A. K. Fedorov, I. L. Kurbakov, Y. E. Shchadilova, and Yu. E. Lozovik, Two-dimensional Bose gas of tilted dipoles: Roton instability and condensate depletion, Phys. Rev. A **90**, 043616 (2014).
[25] C. Mishra and R. Nath, Dipolar condensates with tilted dipoles in a pancake-shaped confinement, Phys. Rev. A **94**, 033633 (2016).

[26] S. Yi and L. You, Trapped atomic condensates with anisotropic interactions, Phys. Rev. A **61**, 041604(R) (2000).

[27] We use the definition of Ref. [5]. Other definitions with a different numerical factor are found in the literature, see for instance, [28,29].

[28] D. C. E. Bortolotti, S. Ronen, J. L. Bohn, and D. Blume, Scattering Length Instability in Dipolar Bose-Einstein Condensates, Phys. Rev. Lett. **97**, 160402 (2006).

[29] M. A. Baranov, M. Dalmonte, G. Pupillo, and P. Zoller, Condensed matter theory of dipolar quantum gases, Chem. Rev. **112**, 5012 (2012).

[30] J. L. Ville, T. Bienaimé, R. Saint-Jalm, L. Corman, M. Aidelsburger, L. Chomaz, K. Kleinlein, D. Perconte, S. Nascimbène, J. Dalibard, and J. Beugnon, Loading and compression of a single two-dimensional Bose gas in an optical accordion, Phys. Rev. A **95**, 013632 (2017).

[31] R. Saint-Jalm, P. C. M. Castilho, É. Le Cerf, B. Bakkali-Hassani, J.-L. Ville, S. Nascimbene, J. Beugnon, and J. Dalibard, Dynamical Symmetry and Breathers in a Two-Dimensional Bose Gas, Phys. Rev. X **9**, 021035 (2019).

[32] D. M. Harber, H. J. Lewandowski, J. M. McGuirk, and E. A. Cornell, Effect of cold collisions on spin coherence and resonance shifts in a magnetically trapped ultracold gas, Phys. Rev. A **66**, 053616 (2002).

[33] The imbalance f is tuned mostly by changing the pulse duration but for small pulses area it is more convenient to also decrease the Rabi frequency to avoid using very short microwave pulses.

[34] E. Timmermans, Phase Separation of Bose-Einstein Condensates, Phys. Rev. Lett. **81**, 5718 (1998).

[35] At nonzero temperature, quantum statistics of thermal bosons lead to multiply this shift by a factor which varies from 1 in the very degenerate regime to 2 for a thermal cloud.

[36] M. J. Martin, M. Bishof, M. D. Swallows, X. Zhang, C. Benko, J. von Stecher, A. V. Gorshkov, A. M. Rey, and J. Ye, A quantum many-body spin system in an optical lattice clock, Science **341**, 632 (2013).

[37] R. J. Fletcher, R. Lopes, J. Man, N. Navon, R. P. Smith, M. W. Zwierlein, and Z. Hadzibabic, Two- and three-body contacts in the unitary Bose gas, Science **355**, 377 (2017).

[38] Y.-Q. Zou, B. Bakkali-Hassani, C. Maury, É. Le Cerf, S. Nascimbene, J. Dalibard, and J. Beugnon, Tan's two-body contact across the superfluid transition of a planar Bose gas, arXiv:2007.12385.

[39] P. A. Altin, G. McDonald, D. Döring, J. E. Debs, T. H. Barter, J. D. Close, N. P. Robins, S. A. Haine, T. M. Hanna, and R. P. Anderson, Optically trapped atom interferometry using the clock transition of large ^{87}Rb Bose-Einstein condensates, New J. Phys. **13**, 065020 (2011).

[40] D. H. J. O'Dell, S. Giovanazzi, and C. Eberlein, Exact Hydrodynamics of a Trapped Dipolar Bose-Einstein Condensate, Phys. Rev. Lett. **92**, 250401 (2004).

[41] J. Stuhler, A. Griesmaier, T. Koch, M. Fattori, T. Pfau, S. Giovanazzi, P. Pedri, and L. Santos, Observation of Dipole-Dipole Interaction in a Degenerate Quantum Gas, Phys. Rev. Lett. **95**, 150406 (2005).

[42] T. Lahaye, T. Koch, B. Fröhlich, M. Fattori, J. Metz, A. Griesmaier, S. Giovanazzi, and T. Pfau, Strong dipolar effects in a quantum ferrofluid, Nature (London) **448**, 672 (2007).

[43] Y. Tang, W. Kao, K. Y. Li, and B. L. Lev, Tuning the Dipole-Dipole Interaction in a Quantum Gas with a Rotating Magnetic Field, Phys. Rev. Lett. **120**, 230401 (2018).

[44] C. J. Pethick and H. Smith, *Bose-Einstein Condensation in Dilute Gases* (Cambridge University Press, Cambridge, England, 2008).

[45] S. Sachdev, *Quantum Phase Transitions* (Cambridge University Press, Cambridge, England, 2006).